Electromechanical Measurements of Plastic Deformation in Polycrystalline Aluminum and Copper

By Akio TAKIMOTO*, Ryoji NISHIHARA**, Hitoshi NAKAO***, Motoshi HIMENO****, Shoji NISHIKAWA***** and Toshiharu SHIMIZU******

(Received July 15, 1982)

Abstract

Electromechanical measurements of plastic deformation phenomena of commercially pure polycrystalline aluminum and copper have been performed at room temperature, where the grain size distribution of test pieces is varied. The room temperature recovery process may reduce their electrical resistivity quite a large percentage, however, some reliable tendencies have been obtained. In aluminum the mechanical hardening curve shows the common tendency and the incremental electrical resistivity varies in two steps with strain up to the instability point in tension. In copper, contrast to the above, both the mechanical hardening and the incremental electrical resistivity curves show common increase with strain. The zero strain electrical resistivity is shown to be inversely proportional to the median of the grain size distribution for aluminum. The incremental electrical resistivity is confirmed to follow the relationship $\triangle\rho/\rho_0=C_1\varepsilon^K$ where the exponential coefficient K is shown to be a function of the median both for aluminum and copper.

Introduction

The variation of electrical resistance associated with elastic deformation has well been determined and has been long employed for engineering use, for example, as a gage factor (K_s). However, the materials having K_s other than 2.0, consequently, show the variation of $d\rho_i/\rho_i$ with strain[1] and the intrinsic resistivity mechanism becomes complex. For deformation up to the plastic range, electrical resistivity of pure metals[2)3)] and special alloys[4)5)] has been investigated mainly to study the relationships between electrical resistivity and the lattice defects such as vacancies, interstitials, and dislocations. The incremental electrical resistivity has thus been given by the proposed relations such as $\triangle\rho\sim\varepsilon^{3/2}$ for vacancies and interstitials, and $\triangle\rho\sim\varepsilon^{1/2}$ for dislocations[6)]. The lattice defects introduced in plastic deformation can be partly or fully annealed out by diffusion and/or annihilation in the process of recovery. Thus, the results will largely depend on the amount of deformation and recovery processes to bring about.

* Department of Industrial Mechanical Engineering
** Graduate School
*** Nippon Oil Seal Industry Co., LTD.
**** Daihatsu Industry Co., LTD.
***** Nissan Automobile Co., LTD.
****** Matsushita Electric Industrial Co., LTD.

We aim to study the relationship between electrical resistivity and plastic strain of commercially pure aluminum and copper and to find if the electromechanical test is beneficial for engineering deformation tests. The plastic strain is, therefore, extended to the instability point in tension and tests are performed at room temperature, where the effect of the recovery process may be a quite large of 50 percent probably[6)7)]. In addition, the effect of the grain size distribution is taken into account.

Experimental Procedure

Polycrystalline pieces of $45\sim50\times2.5\times1.8$ mm^3 were cut out, with the largest length parallel to the rolled direction, from the commercially pure sheet materials of aluminum and copper both having 2 mm thickness. Mechanical steps by filing and polishing were continued to form the piece within the accuracy of ±12.5 and ±5 μm, respectively, in the last two dimensions. Aluminum pieces were annealed for 1 hr. at 350°C to relief mechanically introduced strain and copper ones were done for 1 hr. at 400°C. To get an expected grain distribution, the necessary processes of pre-straining and annealing were repeated on them. The grain distribution of a piece was measured on each of them by the linear analysis method after the final careful surface finishing.

Tensile tests were performed on them by using the developed Adams-type machine at the strain rates of 9.54×10^{-4}sec^{-1} for aluminum and 8.54×10^{-4}sec^{-1} for copper at 20°C. The relatively slender piece was elongated nearly to the instability point with the specially designed tensile jig. Electrical resistance, tensile strain, and the reduction of area were measured at four to eight times during the elongation process, each time by unloading. Electrical resistance was measured carefully with the DC voltage current standard of the type 2853, the current unit of the type 2862 and the precision digital meter of the type 2501 (the minimum digit of 10^{-7}V) in the isothermal room kept its temperature at 20°C and its humidity of $65\pm5\%$. The two current wires were soldered on the two ends of a piece with a special low thermo e.m.f. solder and the voltage wires were connected to copper electrodes whose measuring ends were pointed to get a sharp contact on the surface of the test piece. The measuring pressure working on the electrode was very small and kept to be a constant by a spring device. Consequently, no solder was used for the voltage terminals and the error such as the thermal e.m.f. occuring from soldering was eliminated. The test piece and other necessary devices were again put into another small box of plastics in which the temperature was shut off from a human body and was controlled to be 20 ± 0.0025°C for a short second to get a better approach to the measuring temperature. The current of 1.00000 amp. was set on a test for a very short time to avoid unnecessary heating such as the joule effect, and resistance was thus carefully measured each time.

Resistivity was calculated by the relation, $\rho=RA/L$, where ρ: resistivity, R: measured resistance, A: section area of a piece, and L: the distance between two electrodes. The distance (L) was carefully determined under the measuring microscope and the section area (A) was obtained from the constancy of volume, $\triangle V=0$, in the process of deformation. Of course, the measurement of A was also taken for a

comparison.

Resistivity due to the thermal vibration of the lattice, impurity and substitutional atoms is assumed to be kept unchangeable in the series of this study.

Experimental Results

The plastic flow stress of an engineering polycrystal of the grain diameter (d) can be expressed by the Hall[8] and Petch[9] relation as $\sigma_f=\sigma_0+K'd^{-1/2}$. The flow stress of it having a grain size distribution is no longer able to be expressed by such a simple relation. For the plastic flow strain of it, little information is available except an actual flow stress-strain curve. This study is intended to pick up the mechanical deformation behavior by the electrical device and to get a correlation between them. Electrical resistance measurements have usually been performed on the deformation of some pure metals and special alloys at low temperature and at strain up to the very limited plastic value which is far less than the ultimate strain. We have performed the experiments on polycrystal and multicrystal aluminum and copper of the commercially pure grades at 20°C, and have found interesting relationships between electrical and mechanical properties of them as reported below.

The grain size distribution of aluminum pieces was intentionally varied from that having a very fine grain of nearly 20 μm to that of 20,000 μm which is a bicrystal piece. Three examples of the grain size distribution functions are shown in Fig. 1 which obviously indicates a logarithmic normal distribution given by

$$p\{d\}=\log e(\sqrt{2\pi}\sigma d)^{-1}\exp\{-(\log d-\log d_m)^2/2\sigma^2\}$$

The median (d_m) which is independent of the standard deviation, is employed to express grain size of a piece since the effect of the standard deviation, if any, will be seen as a scatter in the experimental plots later.

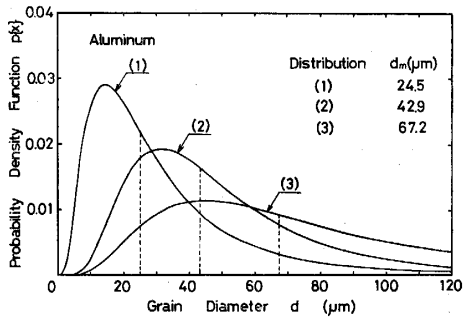

Fig. 1 Three probability density functions of grain diameters, employed for testings, are shown for aluminum. The vertical dotted line is the median in each distribution. $p\{d\}$ is presented as $p\{x\}$ in this figure.

Fig. 2 shows discrete true stress and strain data points for aluminum in which each point corresponds with strain unloaded at and the resistance measurement taken at.

Fig. 2(a) for the group 1 testings contains the results of four polycrystal pieces and a multicrystal piece. Fig. 2(b) is similarly for the group 2 testings of three polycrystal pieces and three multicrystal pieces. The discrete flow curve of data points thus plotted for a piece has been examined to coincide with the continuous flow curve without unloading of the piece of having the same grain size in the preliminary test. The last point in each curve corresponds to the point just before the instability in tension.

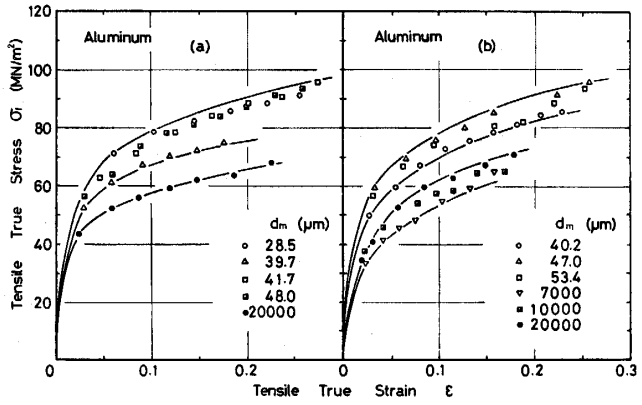

Fig. 2 Tensile true stress and true strain data points of aluminum are shown for two groups. Fig. 2(a) for the group 1 contains the results of five different grain sizes and Fig. 2(b) for the group 2 does those of six different grain sizes.

The zero strain resistivity of aluminum is plotted as a function of the median of grain diameter in Fig. 3. Here the results of polycrystals are shown in Fig. 3(a) and those of multicrystals in Fig. 3(b). In polycrystals the zero strain resistivity decreases with increase in the median of grain size with a scatter band of about 0.03 $\mu\Omega$cm in each median. This scatter band may be due to the effect of the lattice defects which will be widely different for the same median pieces by different pre-straining and annealing conditions as shown next and also to the effect of the standard deviation in the grain distribution. The recovery process occured during the period of experiment might be different for each piece though the one is not strained. Results for multicrystals show a similar tendency with its very mild decrease compared to the ones for polycrystals.

The zero strain resistivity of the pieces having the similar medians is expressed as a function of the annealing time at 550°C in Fig. 4. As the annealing time becomes longer, the zero strain resistivity seems to become lower. and it may be due to the low defect density effect by a long time heating at 550°C. The decrement of about 0.024 $\mu\Omega$cm is given by 25 hour heating. This decrement may correspond with the scatter band in Fig. 3(a). It is the well known fact that electrical resistivity is proportional to the defect density and the defects can be annealed out to decrease the density by a long time heating.

Increase in electrical resistivity ($\triangle\rho$) by straining the different grain size pieces is shown in Fig. 5 for aluminum. As tensile true strain increases, the incremental el-

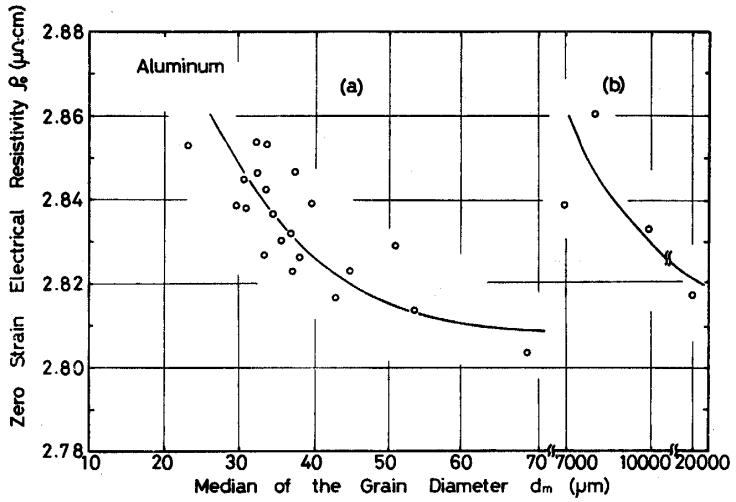

Fig. 3 Decrease in the zero strain electrical resistivity is plotted to increase in the grain diameter of aluminum. Results for polycrystals and multicrystals are shown in Fig. 3(a) and Fig. 3(b), respectively.

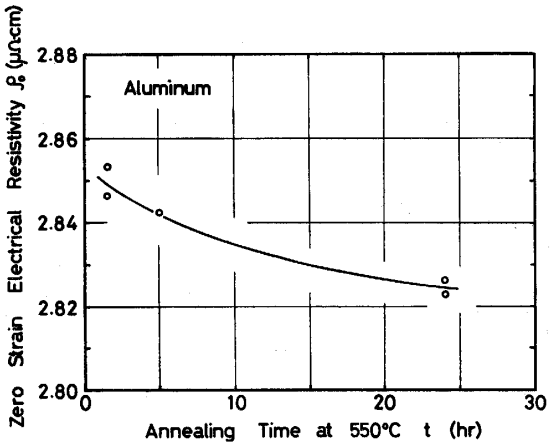

Fig. 4 An example of a relationship between the zero strain electrical resistivity and the annealing time at 550°C. Results for aluminum having the average grain diameter of 32~37 μm are shown.

ectrical resistivity ($\triangle\rho$) increases in two steps having a turning point at around $\varepsilon_p =$ 0.15~0.19. The data points in Fig. 5 have the same meaning as those given in Fig. 2. The results for multicrystal pieces in Fig. 5(b) appear in the low strain range as expected. The magnitude in the incremental electrical resistivity for polycrystals may be decreased by increase in the median of grain size.

For copper, four different grain size distributions are shown in Fig. 6. In annealed copper, quite many annealing twin bands are observed in the microstructure due to its low stacking fault energy of about 40 erg/cm^2. Therefore, we plot two type distribution functions for it, namely the one without twins and the one with twins. The broken lines are the ones without twins and indicate a large difference in the medians

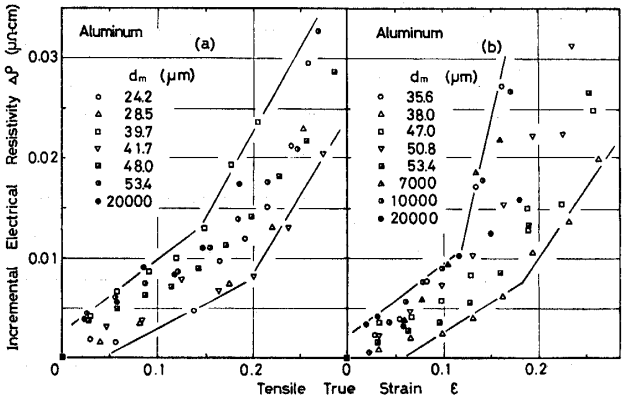

Fig. 5 The increments in electrical resistivity are expressed as functions of tensile strain. Fig. 5(a) for the group 1 contains the data of seven different grain sizes and Fig. 5(b) for the group 2 does those of eight different grain sizes.

in four distributions. The real lines, on the other hand, are the ones with containing twin bands and give a little difference in them. Both distribution functions show the logarithmic normal distribution and the median of each, which is shown by the vertical dotted line, is used to present the grain distribution as predicted in the previous case.

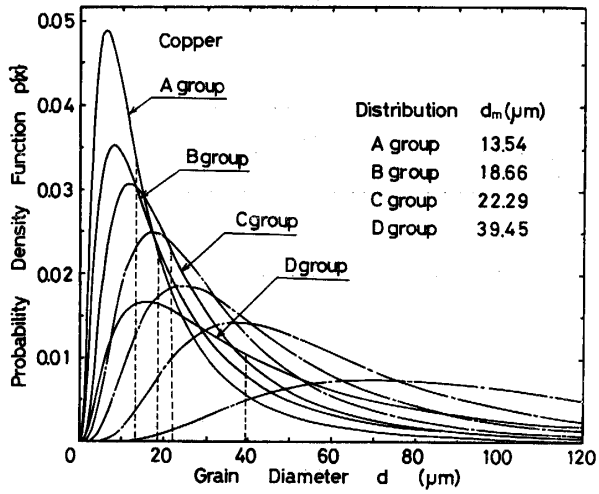

Fig. 6 Eight probability density functions of grain diameter, employed for testings, are shown for copper. The broken lines indicate results without containing twins and the real lines do those with twins. The vertical dotted line is the median in each distribution. $p\{d\}$ is presented as $p\{x\}$ in this figure.

The true stress-strain curves for four different grain pieces are shown in Fig. 7. The Hall and Petch relation is seen except the curve for B and some crossings at small strain are observed. The incremental electrical resistivity ($\triangle\rho$) is plotted to true strain in Fig. 8. The $\triangle\rho$ value increases with the applied true strain up to the point near the instability in tension and the necking phenomena take place at around $\triangle\rho=$

$0.035 \sim 0.040$ $\mu\Omega$cm. This figure contains the results of twelve pieces in three of each distribution and the data points are expressed in a band. The test piece having a smaller median gives a relatively large value of $d(\triangle\rho)/d\,\varepsilon$ in the band.

The microstructures of aluminum and copper pieces are exampled in Photo 1.

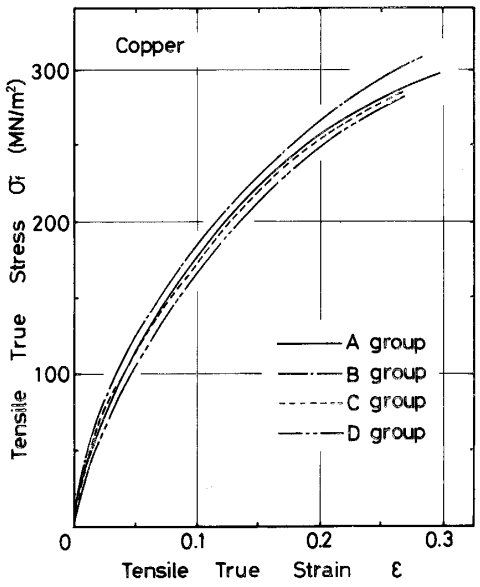

Fig. 7 Tensile true stress and true strain curves for copper of four different grain diameters are shown.

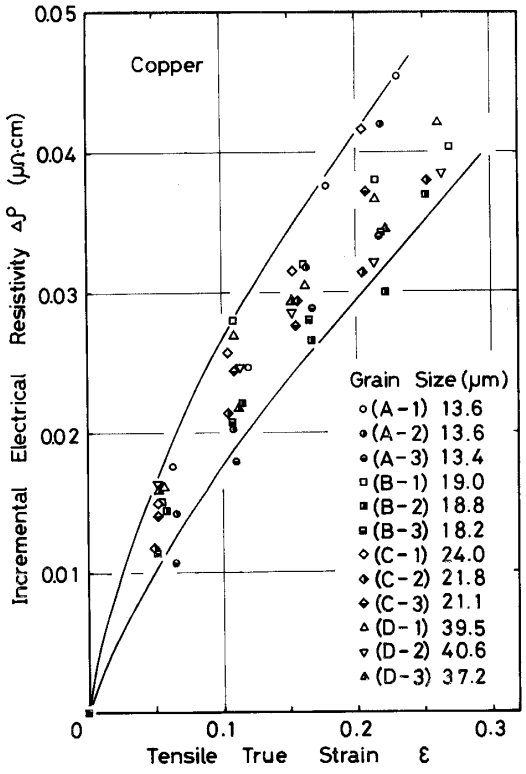

Fig. 8 The increments in electrical resistivity are shown as functions of tensile strain. Results of twelve copper pieces are expressed in the same figure.

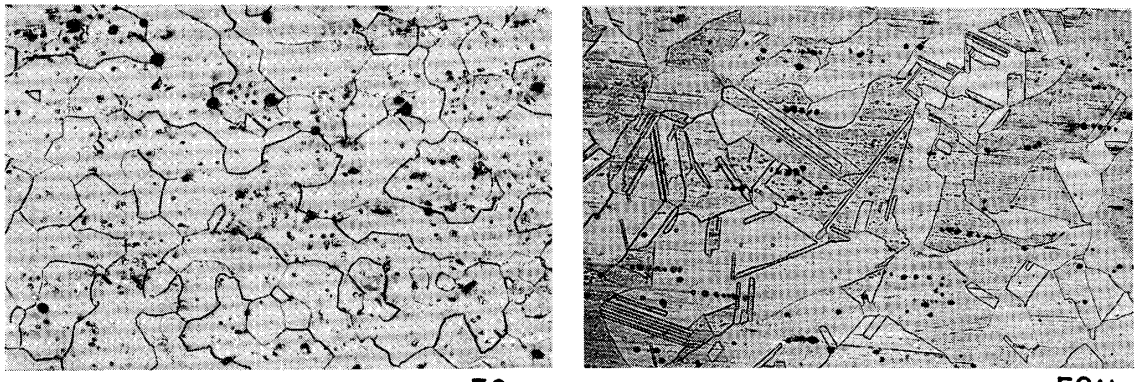

Photo 1 Examples of microphotographs of aluminum 1(a) and copper 1(b) pieces employed for testings. Photo 1(a) of $d_m \fallingdotseq 29.53$ μm with no twin bands in each grain and photo 1(b) of $d_m \fallingdotseq 18.20$ μm containing twin bands in most grains (the d_m with no twin bands is nearly equal to 36.32 μm).

Photo 1(a) is for an aluminum piece of $d_m \fallingdotseq 29.53$ μm and Photo 1(b) is for a copper piece of $d_m \fallingdotseq 18.20$ μm.

Discussion

Electrical resistivity is inversely proportional to the effective number of the free electrons per unit volume and is proportional to the scattering probability of them.[19] The lattice defects which are stable at room temperature, will accordingly increase the latter and will result in the increase in electrical resistivity except the cases observed in the special phenomena of deformation in Au–Pd[10] and Cu–Pd[11] alloys and the strain induced martensitic transformation[12][13] in Fe–Ni–C and Fe–Ni–Co–C alloys. Mechanical factors such as stress and strain are also dependent on the lattice defects, but they may not be so keen as electrical resistivity. Here we discuss some correlations between electrical and mechanical properties which are related to the lattice defects and tensile deformation.

The Grain Boundary

Lattice arrangements in the grain boundary are, of cource, out of order and the scattering of an electron will be increased. The grain boundary contribusion to electrical resistivity will increase as grain size decreases. This tendency is clearly observed in Fig. 3 with an aid of Photo 1(a) for aluminum. The zero strain electrical resistivity for polycrystals in Fig. 3(a) shows a quite obvious dependence on the median compared with the results in Fig. 3(b) for multicrystals where the scattering due to the grain boundary may not be a primary factor since the 7,000 μm piece has about 6 grains and the 20,000 μm piece does only 2 grains in the gauge section of the test piece, respectively. A similar dependence on grain size has been also reported by a Russian investigator[14] on aluminum alloys.

Grain Size and the Lattice Defects

Mechanical stress is dependent on the grain diameter by the Hall and Petch relation, that is, $\sigma_f \propto K' d^{-1/2}$ and on the dislocation density (ρ_d) by the relation, $\tau \propto \alpha G b \sqrt{\rho_d}$. The dislocation density is also inversely proportional to an average inter-dislocation distance (l). All these relations may predict flow stress of the polycrystalline materials. Actual deformation phenomena are not often so, and the dislocation density in a grain should be considered to be composed of two parts[15][16], that are the geometrically necessary dislocation density (ρ^G) and the statistical dislocation density (ρ^S), where the total dislocation density is $\rho^T = \rho^G + \rho^S$. In a small grain, ρ^G will dominate up to a large plastic strain and in a large grain ρ^S overcomes ρ^G after some plastic strain.

Stress and strain curves of aluminum in Fig. 2 are understood to follow the Hall and Petch relation except a few examples. The incremental electrical resistivity in Fig. 5 may indicate the effect of deformation mechanism more precisely showing two steps in the increment, namely a relatively mild step up to $\varepsilon_P = 0.15 \sim 0.19$ and a relatively steep step up to the instability point if the relative effect of the room tem-

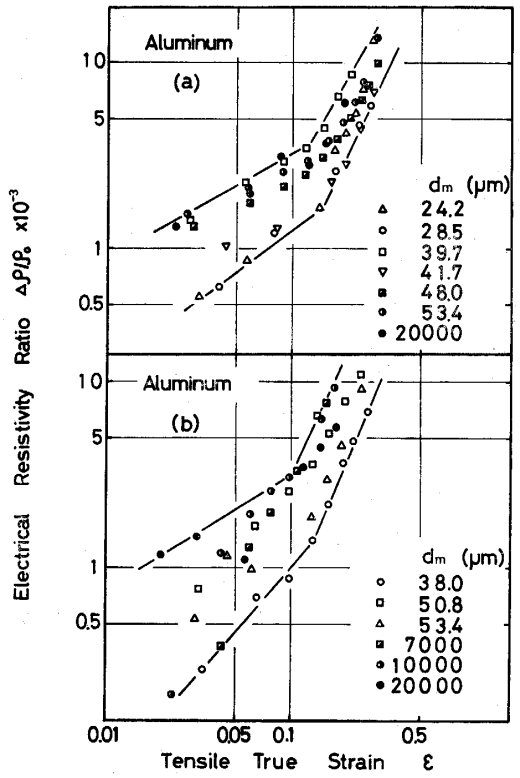

Fig. 9 Increase in the electrical resistivity ratio is plotted to tensile true strain. Fig. 9(a) for the group 1 contains the data of seven different grain sizes and Fig. 9(b) for the group 2 does those of six different grain sizes.

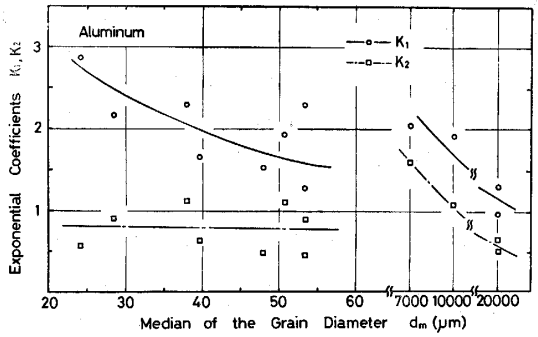

Fig. 10 The relationships between the exponential coefficients (K_1, K_2) and the median of a grain distribution are given for aluminum. Results for polycrystals and multicrystals are shown in Fig. 10(a) and Fig. 10(b), respectively.

perature recovery is assumed to be the same for each strain. These two steps correspond with the different deformation mechanism which may be connected with the competition of the two different groups of dislocation densities mentioned above though no qualitative evidence is available, and especially the latter step may be related with the dominating ρ^S and the multiple slip mechanism in a large strain. To determine these two steps qualitatively, the relation proposed by Van Bueren[17],

$$\triangle\rho = C\varepsilon^K$$

is modified as

$$\triangle\rho/\rho_0 = (C/\rho_0)\varepsilon^K = C_1\varepsilon^K$$

and taking its logarithm it becomes as

$$\log(\triangle\rho/\rho_0) = \log C_1 + K\log\varepsilon$$

The results in Fig. 5, with each ρ_0, are shown as in Fig. 9. The exponential constants K_1 and K_2 are calculated and given as functions of the median in Fig. 10 for aluminum. The data indicate that K_1 is dependent on the median and K_2 is a nearly constant,

showing a steeper slope for a smaller median which is seemed to be a right trend from the above discussion on the dislocation density for polycrystals. In a case of copper, the situation is a little different. First, this material has conduction electrons of one or two in the solid metal (some atoms have different numbers of conduction electrons in between the free atoms and the solid metals) compared with those of three in aluminum. However, electrical resistivity of copper is, in fact, nearly 60~61% of that of aluminum. Second, copper has the low stacking fault energy of roughly 40 erg/cm^2 [18] which is about one-fifth of that of aluminum and easily contains the annealing twin in a grain and this twin boundary may take part in the phenomena experimented. The grain size distributions are therefore expressed in two ways of without twins and of with twins as in Fig. 6. Stress and strain curves in Fig. 7 and the incremental electrical resistivity in Fig. 8 are obviously expressed better with that containing twin bands since so much difference is not observed in the mechanical and electrical properties, respectively, as we can see the difference in the grain size distributions without twins in Fig. 6. In Fig. 8 the relative effect of the recovery process at room temperature is assumed to be again the same for each strain. The twin boundary is thus sensitive to both properties. The incremental electrical resistivity ratio ($\triangle\rho/\rho_0$) is expressed as a function of strain in Fig. 11 for copper and the exponential constant (K) is calculated for each grain distribution. The result of this is shown in Fig. 12 and again K decreases with increase in the median for copper. The two deformation steps in aluminum and the one step in copper may be more clearly understood if we realize the fact that the different dislocation slip length (l) in both metals is taken into account, where l is, for example, about 3~4 μm at 0.2%ε_p for aluminum of 20~200 μm diameter grains and that is 10~20 μm at 0.2%ε_p for copper of 15~150 μm diameter grains.

Plastic Strain and Electrical Resistivity

As we have mentioned in the begining, electrical resistivity is dependent upon the

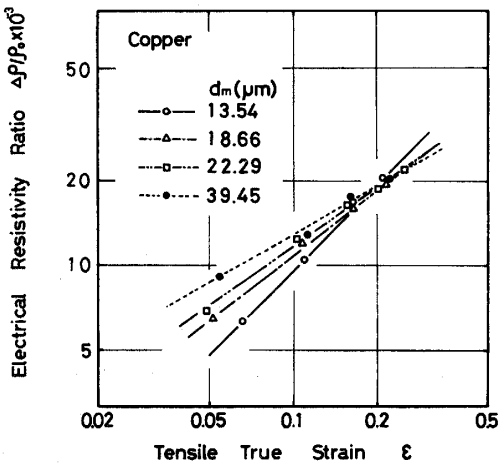

Fig. 11 Increase in the electrical resistivity ratio is plotted to tensile true strain for copper.

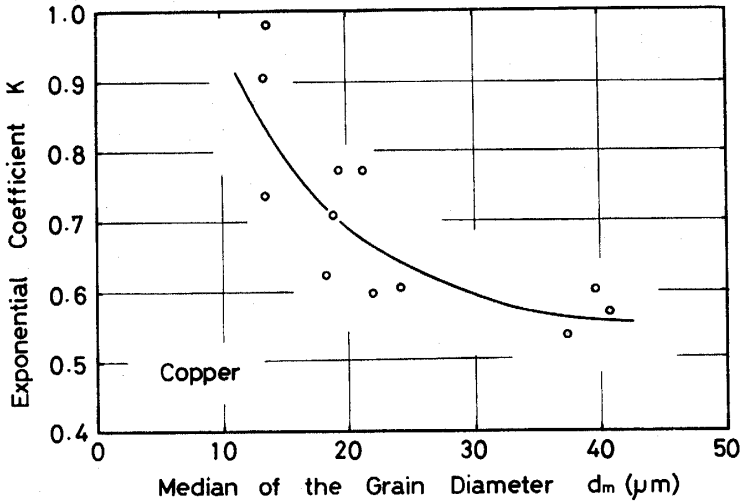

Fig. 12 A relationship between the exponential coefficient and the median of a grain distribution is given for copper.

effective number of the free electrons per unit volume and the scattering probability which is sensitive to the various lattice defects. However, the recovery processes, as for copper at least five stages[7] reported, will also take place to reduce the lattice defects, whose relative effect is assumed to be the same for each strain here. Therefore, for engineering materials having the small number of the effective free electrons per unit volume, large effects of lattice defects and less recovery effects at room temperature the electrical resistivity measurement may be useful in place of mechanical measurements such as stress and strain. In this study the first and second conditions are satisfied with

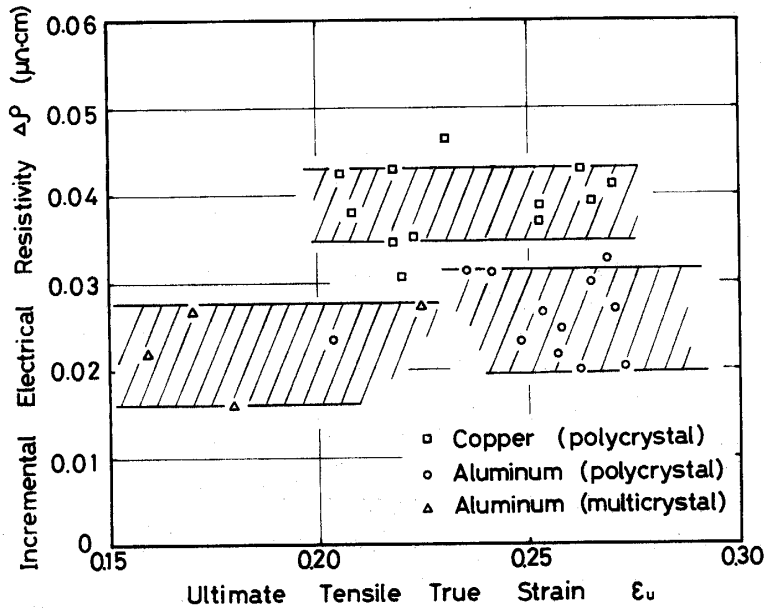

Fig. 13 The relationships between the incremental electrical resistivity and plastic strain just before the tensile instability point are shown both for aluminum and copper.

engineering aluminum and copper but the third condition is seemed to be a little bit strong. The effect of the room temperature recovery will be stronger in aluminum than in copper since the former has a lower limit of the recrystallization temperature. However, it is proved here that the some strained state may possibly be electrically checked up even at room temperature if the electrical device has good enough accuracy. Such an example of electrical check up at around the instability points in tension is given in Fig. 13. The figure indicates that polycrystalline copper pieces approach to the instability point at around 4×10^{-2} $\mu\Omega$cm and polycrystalline aluminum pieces do at around 2.5×10^{-2} $\mu\Omega$cm and multicrystal aluminum pieces do at around 2.0×10^{-2} $\mu\Omega$cm. These are the limitations which the materials can afford in tension.

Conclusions

Electromechanical tests under tension have been performed on commercially pure polycrystalline aluminum and copper at room temperature, where the grain size distribution of test pieces is varied. The following items are concluded.

(1) The grain size distribution is a logarithmic normal curve for both metals, and the one containing twin bands corresponds better with the electrical and mechanical properties of copper.

(2) The zero strain electrical resistivity of aluminum is shown to be inversely proportional to the median of grain size.

(3) The incremental electrical resistivity is confirmed to follow the relationship $\Delta\rho/\rho_0=C_1\varepsilon^K$ where the exponential coefficient is shown to be a decreasing function of the median both for aluminum and copper.

(4) The incremental electrical resistivities at around the instability point in tension are 2.5×10^{-2} and 4×10^{-2} $\mu\Omega$cm for polycrystalline aluminum and copper, respectively.

References

1) Richards, W. "Engineering Materials Science" (Wads Worth, San Francisco) p. 422
2) Martin, M. C. and Welton, K. F. Acta Met. **15**, 571–573 (1967)
3) Schrank, J., Zehetbauer, M., Pfeiler, W. and Trieb, L. Scripta Met. **14**, 1125–1128 (1980)
4) Saito, K. and Tsujimoto, T. Journal of Japan Institute of Metals **35**, 764–769 (1971) (in Japanese)
5) Hibbard, Jr. W. R. Acta Met. **7**, 565–574 (1959)
6) Van Bueren, H. G. Acta Met. **1**, 607–609 (1953)
7) Seeger, A. "Encyclopedia of Physics VII/1" (Springer-Verlag) p. 431–476 (1955)
8) Hall, E. O. Proc. Phys. Soc. London **643**, 747– (1951)
9) Petch, E. O. J. Iron Steel Inst. London **173**, 25– (1953)
10) Logie, H. J., Jackson, J., Anderson, J. C. and Nabarro, F. R. N. Acta Met. **9**, 707–713 (1960)
11) Jaumot, F. E. and Sawatzkl, A. Acta Met. **4**, 126–144 (1953)
12) Takimoto, A., Nishihara, R. and Shoda, S. Proc. Symposium Japan Institute of Metals, Lecture Meeting (1981 Nov.) 69 (in Japanese)
13) Takimoto, A., Nishihara, R. and Shoda, S. Proc. Symposium Japan Institute of Metals, Lecture Meeting (1982 Apr.) 163 (in Japanese)

14) Панько, Т.И., Зайковская, П.В. and Вангенгейм, С.Д. Metallofizika (SUN) 3, [3], 113–118 (1981)
15) Ashby, M. F. Phil. Mag. **21**, 399–424 (1970)
16) Thompson, A. W., Baskes, M. I. and Flanagan, W. F. Acta Met. **21**, 1017–1028 (1973)
17) Van Bueren, H. G. Philips Res. Rep. **12**, 1–190 (1957)
18) Suzuki, H. "Teniron Nyumon" (AGNE, Tokyo) p. 161 (1980) (in Japanese)
19) Mott, N. F. and Jones, H. "The Theory of the Properties of Metals and Alloys" (Dover, New York) p. 248– (1958)